Journal of Hydrology: Regional Studies 27 (2020) 100644

Contents lists available at ScienceDirect

Journal of Hydrology: Regional Studies

journal homepage: www.elsevier.com/locate/ejrh

Between boreal Siberia and arid Central Asia – Stable isotope hydrology and water budget of Burabay National Nature Park ecotone (Northern Kazakhstan)

Vadim Yapiyev[a,b,c,*], Grzegorz Skrzypek[d], Anne Verhoef[c], David Macdonald[e], Zhanay Sagintayev[a,f]

[a] Department of Civil and Environmental Engineering, School of Engineering, Nazarbayev University, 53 Kabanbay Batyr Ave, Nur-Sultan, 010000, Kazakhstan
[b] National Laboratory Astana, Nazarbayev University, Nur-Sultan, Kazakhstan
[c] Department of Geography and Environmental Science, The University of Reading, Reading, United Kingdom
[d] West Australian Biogeochemistry Centre and Ecosystems Research Group, School of Biological Sciences (M090), The University of Western Australia, 35 Stirling Highway, Perth, WA 6009, Australia
[e] British Geological Survey, Wallingford, Oxfordshire, United Kingdom
[f] The Environment & Resource Efficiency Cluster (EREC), Nazarbayev University, Kazakhstan

ARTICLE INFO

Keywords:
Endorheic lake
Evaporation
Fill and spill
Water balance
Stable isotopes
Groundwater

ABSTRACT

Study region: Burabay National Nature Park (BNNP) of North Kazakhstan is located between humid boreal forests and an arid steppe of Central Asia.
Study focus: The stable hydrogen and oxygen isotope analyses of precipitation, stream, lake and ground waters were used for water budget calculations of the BNNP endorheic lake system to assess the impact of increasing aridity on lakes in this most continental part of the Earth.
New hydrological insights for the region: The stable isotope results confirmed two different types of lakes in BNNP: Burabay and Shortandy Lakes are more similar to higher latitude lakes (e.g. South Siberia), while Kishi and Ulken Shabakty Lakes are more comparable to the steppe lakes of Central Asia. The slopes of evaporation lines for this region, obtained by regression analysis of lake water samples, ranged from 4.57 (steppe lakes) to 6.21 (forest lakes). The evaporation over inflow ratios (0.34 Burabay, 0.69 Ulken Shabakty, and 0.53 Shortandy) are in good agreement with catchment water budget calculations reflecting different groundwater inputs and water retention times. The recent water level rise in the Ulken Shabakty Lake terminal basin was observed for the first time in a decade. This increase can be explained by the 'fill and spill' hypothesis and suggest that a single unusually wet year may significantly replenish water resources despite long-term increasing aridity of the region.

1. Introduction

The quantification of hydrological processes governing the water balance of lakes is a challenging task, especially in lake systems with heterogeneous geology and complex climate controls. In most areas, especially in cold semi-arid regions, there are two critical processes determining lake hydrology: 1) open water evaporation, and 2) lateral inflow/outflow of shallow groundwater and surface

* Corresponding author at: Department of Geography and Environmental Science, The University of Reading, Reading, United Kingdom.
E-mail address: vyapiyev@nu.edu.kz (V. Yapiyev).

https://doi.org/10.1016/j.ejrh.2019.100644
Received 2 July 2019; Received in revised form 6 October 2019; Accepted 16 November 2019
Available online 10 December 2019

water to lakes. Both evaporation and groundwater flows are the 'invisible' fluxes that are difficult to quantify. In addition, in arid and semi-arid environments, open water evaporation is frequently the dominant factor determining the water loss in lakes.

Lake evaporation is usually estimated applying micrometeorological equations such as the Penman method driven by local weather data (McMahon et al., 2013). The results of the theoretical calculations are often verified by pan evaporation observation or micrometeorological measurements in the field (Finch and Calver, 2008; McJannet et al., 2017; McMahon et al., 2013) using eddy-covariance equipment mounted downwind of the lakes on 'flux towers' or installed on the lake on buoys, vessels or small islands (Xiao et al., 2018).

The lateral interactions of groundwater with lakes can be measured directly using groundwater seepage meters (Ala-aho et al., 2013; Boyle, 1994) but are usually investigated with measurements of hydraulic potentials in the watershed subsurface system combined with numerical modeling tools (Krabbenhoft et al., 1994; Shaw et al., 2013). These traditional methods require constant long term monitoring of vapor fluxes or water levels, as well as detailed information on subsurface and aquifer parameters. These data are notoriously difficult to obtain in geologically heterogeneous watersheds, in particular in remote locations. Hence, these methods are logistically and methodologically challenging, time-consuming and costly. The alternative tracer methods, such as the analysis of the stable hydrogen and oxygen isotope composition of water (stable water isotopes - SWI) have been widely utilized in lake water balance studies to identify both the evaporative losses and groundwater inputs on all continents (Gibson et al., 2008). However, only a few studies using this approach have been conducted to improve the understanding of lake water budgets in Central Asia. Therefore, SWI data are very limited for surface waters, groundwaters, and precipitation in Central Asia, a region that is subjected to the most continental climate globally (Sun et al., 2017; Wang et al., 2016). Mizota et al. (2009) in their study of the Lake Chany complex in western Siberia based on water stable hydrogen and oxygen isotopes and stable sulfur isotope compositions, concluded that increasing salinity for these lakes is primarily driven by direct lake water evaporation. Oberhänsli et al. (2009) estimated the water budget of the Aral Sea using SWI, and confirmed that both evaporative losses and groundwater inflows are significant water balance components for this large lake that has suffered a considerable decline in water levels since the 1960s (Micklin, 2016). Ma et al. (2018) recently reported SWI composition of the large high-altitude basin of Issyk-Kul Lake, inferring intensive surface water evaporation under low relative humidity.

Lakes in arid Central Asia are particularly vulnerable to climate change and their water levels are in decline (Pekel et al., 2016; Yapiyev et al., 2017a). In this study, we present our conclusions on water budget changes in a series of lakes located in the endorheic watersheds of Burabay National Nature Park (BNNP) in the cold semi-arid part of Northern Central Asia (Kazakhstan), and which reflect continental conditions for the region located between boreal Siberia and arid Central Asia. Previous studies provided a deeper understanding of the drivers of the lake level fluctuations observed in BNNP over the last 100 years (Yapiyev et al., 2019, 2017b). The main purpose of the current study was to a) verify our previous long-term observations and improve the BNNP lake water budgets using the stable isotope mass balance (IMB), and b) identify hydrological connectivity and lateral interactions of lakes with their watersheds using stable isotopic tracers. The overarching aim of this study was to improve our understanding of water cycle in this under-researched cold semi-arid environment of Central Asia.

2. Theory

2.1. Stable isotope mass balance

The water balance of a well-mixed lake under steady-state conditions (no significant water volume reductions) can be estimated from the stable isotope mass balance (IMB) model:

$$I_L = Q_L + E_L\,(\mathrm{m^3 s^{-1}}) \tag{1}$$

$$\delta_\mathrm{I} = \delta_\mathrm{q} + \delta_\mathrm{E}\,(‰) \tag{2}$$

Where: I_L is all water inputs to the lake (surface and groundwater inflow from the catchment and precipitation over the lake), Q_L is surface or groundwater outflow from the lake, E_L is lake evaporation; δ_I, $\delta_\mathrm{q}$andδ_E are the stable isotope compositions of inflow, outflow and evaporation flux (Gibson et al., 2017; Yi et al., 2008). For a typical well-mixed lake under steady conditions, we can assume that $\delta_q \approx \delta_L$ (see (Gibson et al., 2016; Yi et al., 2008) for details), where δ_L is the isotopic composition of the lake. With this substitution in Eq. 2, we can estimate evaporation over inflow ratio (E_L/I_L) using only isotopic compositions of water balance components:

$$\frac{E_L}{I_L} = \frac{\delta_\mathrm{I} - \delta_\mathrm{L}}{\delta_\mathrm{E} - \delta_\mathrm{L}}(\text{dimensionless}) \tag{3}$$

While δ_L can be measured by sampling lake or outflowing water and δ_I can be estimated from isotopic analysis of precipitation and the other water inflows to the lake, δ_E can only be estimated indirectly. The evaporative signature of vapors (δ_E) from a reservoir, such as a lake, for a particular period, can be estimated using the Craig-Gordon model (Craig and Gordon, 1965; Gibson et al., 2016; Yi et al., 2008):

$$\delta_\mathrm{E} = \frac{(\delta_\mathrm{L} - \varepsilon^+)\alpha^+ - \mathrm{h}\delta_\mathrm{a} - \varepsilon_\mathrm{K})}{(1 - \mathrm{h} + 10^{-3}\varepsilon_\mathrm{K})}(‰) \tag{4}$$

Here h is the relative humidity of the atmosphere (as fraction), δ_a is the stable isotope composition of atmospheric moisture that can

be defined as $\delta_a = (\delta_P - \varepsilon^+)/\alpha^+$, where δ_P is the isotopic composition of precipitation, ε^+ is the temperature dependent equilibrium isotope separation given as $\varepsilon^+ = (\alpha^+ - 1) \times 1000$ (Horita and Wesolowski, 1994; Skrzypek et al., 2015), α^+ is the equilibrium isotope fractionation which is also temperature dependent (see Horita and Wesolowski, 1994; Skrzypek et al., 2015), and ε_K is the kinetic isotopic fractionation, defined as $\varepsilon_K = (1 - h) \times C_k$, where C_k is kinetic separation constant: 12.5‰ for δ^2H and 14.2‰ for δ^{18}O (Gonfiantini, 1986; Horita et al., 2008). Note in Eq. 4, h and ε are in decimal notation.

By combining Eqs. 3 and 4 following Gibson and Reid (2014), we find:

$$\frac{E_L}{I_L} = \frac{\delta_L - \delta_I}{m \times (\delta^* - \delta_L)} \tag{5}$$

where m is a dimensionless calculation factor:

$$m = \frac{(h - \frac{\varepsilon}{1000})}{(1 - h + \frac{\varepsilon_K}{1000})} \tag{6}$$

with ε the total fractionation factor:

$$\varepsilon = \frac{\varepsilon^+}{\alpha^+} + \varepsilon_K \tag{7}$$

and δ^* is the limiting stable isotope composition enrichment (the threshold defining the limit of isotopic enrichment by evaporation):

$$\delta^* = \frac{(h \times \delta_a + \varepsilon)}{(h - \frac{\varepsilon}{1000})} \tag{8}$$

2.2. Local evaporation lines

The stable isotope composition of water derived from the lakes in a particular region plotted in δ^{18}O vs. δ^2H space defines the local evaporation line (LEL). Strictly speaking this is an approximation; a LEL is a 'true' evaporation line if there are no other water inputs apart from direct precipitation over the lake. The LELs are usually derived by fitting the surface water sample data using regression analysis. However, LEL slopes (S_{LEL}) can be calculated theoretically based on SWI data (such as surface water, atmospheric composition, and precipitation) and relative humidity (Gat, 1995; Gibson et al., 2008). S_{LEL} is primarily a function of humidity and ambient moisture stable isotope composition. There are two common formulations to calculate S_{LEL}: 1) Gat (1998), Eq. 9, and 2) predicted by the Craig-Gordon model (Gibson et al., 2008), Eq. 10:

$$S_{LEL1} = \frac{[h(\delta_a - \delta_L) + \varepsilon]_{2H}}{[h(\delta_a - \delta_L) + \varepsilon]_{18O}} \tag{9}$$

$$S_{LEL2} = \frac{\left[\frac{h(10^{-3}\delta_a - 10^{-3}\delta_P) + (1 + 10^{-3}\delta_P)10^{-3}\varepsilon}{h - 10^{-3}\varepsilon}\right]_{2H}}{\left[\frac{h(10^{-3}\delta_a - 10^{-3}\delta_P) + (1 + 10^{-3}\delta_P)10^{-3}\varepsilon}{h - 10^{-3}\varepsilon}\right]_{18O}} \tag{10}$$

where all variables are as described above (note in Eqs. 9 and 10 h is given as a fraction). Gat's equation (S_{LEL1}, Eq. 9) takes into account both the isotopic composition of the ambient atmosphere (δ_a) and lake water (δ_L) while Eq. 10 (S_{LEL2}) uses δ_a and δ_P. Thus S_{LEL2} depends on atmospheric conditions only, while S_{LEL1} is influenced by the isotopic composition of lake water and reflects different inputs such as snowmelt and groundwater. The S_{LEL} for the lakes in temperate regions usually ranges from 4 to 6 (Gibson et al., 2008).

3. Materials and methods

3.1. Study site

BNNP is located in northern Kazakhstan (53 °N, 70 °E, 300–400 msl, see Fig. 1a). The climate in BNNP is cold semi-arid with the snow cover period lasting from mid-November to mid-April. Long-term (1986–2016) potential evapotranspiration (*PET*) is ~750 mm year^{-1} and precipitation (*P*) is ~330 mm year^{-1} (Yapiyev et al., 2019, 2017b). Thus the aridity index (*AI*), defined as the ratio of mean annual *P* to mean annual *PET*, is 0.44. Climatologically BNNP belongs to the transition zone between cold energy-limited northern Siberia and the water-limited drylands of Central Asia. The BNNP area is dominated by westerly winds that are characteristic for wider northern Central Asia (Yapiyev et al., 2017b). Air temperature and precipitation peak in July (summer mean ~17 °C, in Shuchinsk, see Fig. 1a). The summer precipitation (constituting around half of the annual total) for this region mostly comes from recycled evaporation derived from winter precipitation in continental Eurasia located to the west and the north (Numaguti, 1999). BNNP catchments are in the Esil-Tobyl river basin draining into the Irtysh River in the Ob River basin (Yapiyev et al., 2019, 2017b).

The Kokshetau ridge encircling the study area creates conditions for higher precipitation relative to the surrounding flat steppe;

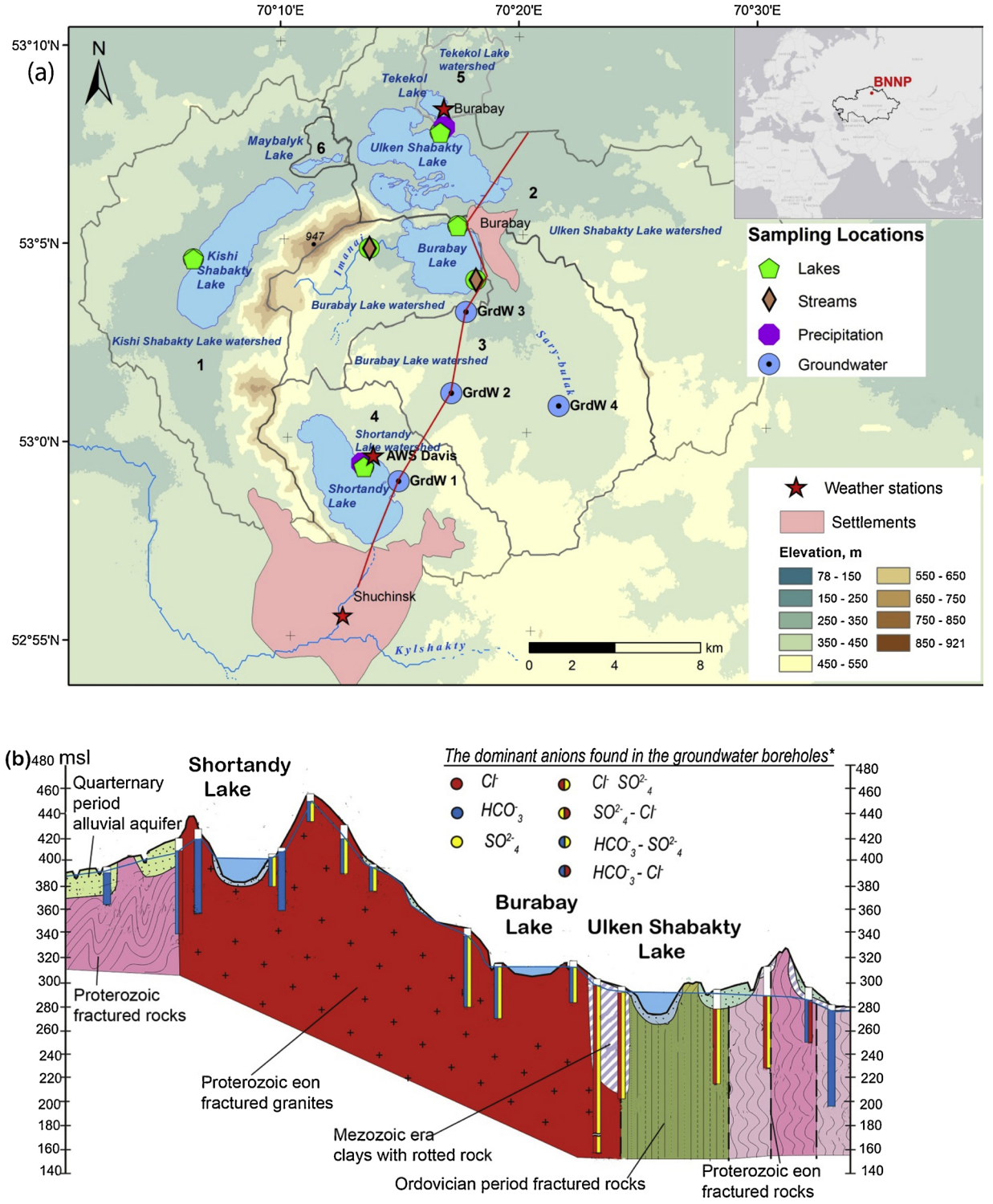

Fig. 1. (a) Burabay National Nature Park location and main lake catchments. The weather stations, SWI (stable water isotopes) sampling sites, groundwater monitoring boreholes (GrdW), as well as local settlements. The sampling locations are presented by different symbols as per the legend. The solid red line shows location of the hydrogeological cross-section (the map is adapted from Yapiyev et al., 2017b); **(b)** Hydrogeological cross-section with location of lakes and the aquifers, vertical axis labeled with elevation (msl), dominant anions found groundwater boreholes (adapted from Dosumov et al., 2014)*.

Table 1
Some characteristics of the four BNNP lakes.

Lake	Lake Surface Area, SA_L (km^2)	Catchment Area, SA_C (km^2)	Ratio Catchment/Lake Surface Area, r_{SA}	Salinity ($g\ L^{-1}$)	Max. Depth (m)	Average Depth (m)	Lake Volume, V_L[3](GL)
Kishi Shabakty	16.79[1]	139[2]	8.2[2]	4.2-4.6[2]	12.0[2]	6.6[2]	112[2]
Ulken Shabakty	18.04[1]	150[2]	8.15[1] (3.15)[1]*	0.8-0.9[2]	25[2]	8.68[1]	166.01[1]
Burabay	10.00[1]	164[2]	16.4[1]	0.1-0.2[2]	5.4[1]	3.14[1]	31.33[1]
Shortandy	14.70[1]	70[2]	4.76[1]	0.2-0.3[2]	22.2[1]	11.85[1]	179.35[1]

Data sources: [1] (Yapiyev et al., 2019), [2] (Yapiyev et al., 2017b), [3] for 2016.
*for 2016, **This ratio is based on a reduced catchment area (see section 4.4 in (Yapiyev et al., 2019) for details).

the ridge acts as a small 'water tower' encouraging orographic rainfall (Yapiyev et al., 2017b). BNNP lakes have tectonic origins and differ from the common pan lakes found in the surrounding region (see also Fig. 1b). In this study, we investigated four lakes: Burabay, Shortandy, Kishi Shabakty and Ulken Shabakty (Table 1, Fig. 1). Burabay and Shortandy are freshwater forest lakes; Ulken and Kishi Shabakty have more distinct features of steppe lakes with higher salinity, see Table 1, (Yapiyev et al., 2017b). Limnologically, BNNP lakes can be classified as cold continuous polymictic (Uryvaev, 1959). The nature of these lakes, which are well-mixed throughout the year, makes them particularly suitable for a stable isotope study (Brooks et al., 2014).

3.2. Sampling design

The water samples for SWI analyses (54 in total, see Table 3) were collected during one hydrologic year from November 2015 to November 2016. Lake water samples were collected approximately each month during the ice-free period to the capture evaporation signal and groundwater streamwater samples were collected quarterly. The water samples were collected in duplicate for each site, in 20 mL borosilicate glass scintillation vials with screw caps (Wheaton Science Products, USA, Part no. 986542). Immediately after collection, all samples were sealed with Parafilm M (Bemis Company, USA, Part no. PM-992) to avoid evaporation. The samples were stored at room temperature until analysis. The lake water samples were collected by grab sampling at the shoreline at fixed locations (see Table 3 and Fig. 1a). The lake water was sampled at approximately monthly intervals, from the start of the open water season (end of April) to the first days of November 2016 (which was about one week before permanent ice-cover; ice-on). Snow samples collected near Lake Shortandy (Fig.1a, near AWS Davis) were melted in a sealed container at room temperature. Rainfall samples were collected at Kazakh State Hydrometeorological Agency (Kazhydromet) weather station near Ulken Shabakty Lake (Fig. 1a, sampling point 'Burabay'). The rainfall samples were collected during abundant precipitation events using a large plastic container and immediately transferred into the vials and sealed. Groundwater samples were collected from boreholes (GrdW1-4, Fig. 1a) using a bailer. Groundwater was sampled during the open water season at approximately three-month intervals (end of April, mid-July, and end of October 2016). Stream samples (Fig. 1a) were collected at approximately the same times as groundwater samples following the same sampling procedure used for lake water samples. Prior to analysis, all samples were stored in the dark at room temperature.

3.3. Stable isotope analyses of water

Before analysis, the samples were filtered into 2 mL screw-top vials with PTFE caps (Thermo Scientific, Chromacol, USA, part no 2-CV(A)ST-CP) through a disposable hydrophilic 0.45 μm PTFE syringe filter (Millex, Merc Millipore, Ireland, part no SLCR025NS) to remove suspended impurities. The samples were analyzed at the Global Institute for Water Security, McDonnell Watershed Hydrology Laboratory (Saskatchewan, Canada) on a Liquid Water Isotope Analyzer (Los Gatos Research). The analyzer uses liquid water Off-Axis Integrated-Cavity Output Spectroscopy (Off-Axis ICOS) and has an uncertainty of $\leq \pm 1.0$ for δ^2H and ± 0.2 for $\delta^{18}O$. The following reference materials were used to normalize obtained values to VSMOW international scale: 'Saskatoon Snow Melt Water' (SSMW): $\delta^2H = -200.4‰$, $\delta^{18}O = -26.1‰$; and 'Enriched': $\delta^2H = 3.2‰$, $\delta^{18}O = -0.3‰$). All samples were tested for volatile organic compound contamination with Los Gatos Research's Spectral Contamination software. All values are reported as parts per thousand (‰) according to the Vienna Standard Mean Ocean Water - Standard Light Antarctic Precipitation (VSMOW-SLAP) scales.

3.4. Hydrometeorological and groundwater data

Relative humidity and air temperature for 2016 were recorded by Kazhydromet (Kazakh State Hydrometeorological Agency) weather station located on the northern shore of Ulken Shabakty Lake (see Fig. 1a, 'Burabay' weather station). Kazhydromet also surveys lake water levels taking measurements daily at 8:00 and 20:00 in Lakes Burabay, Shortandy and Ulken Shabakty using a graduated vertical staff gauge and a geodetic level referencing to a gauge datum (Mean Sea Level, msl, WGS84).

A wireless automatic weather station (AWS) Vantage Pro2 Plus model 6163 (Davis Instruments, Inc.) with integrated sensor suite was installed in November 2013 on the shore of Shortandy Lake (52°59′19.87″N, 70°13′6.48″E; Fig. 1a). The station was mounted 3 m high on a metal pole and had the wireless console. The AWS was equipped with the following sensors: tipping bucket rain gauge (0.2 mm accuracy), air temperature probe (housed in fan-aspiration radiation shield), relative humidity sensor, a solar radiation sensor, cup anemometer for wind direction and speed (all sensors manufactured by Davis Instruments, Inc.). Measurements were

recorded at 30-minute intervals and averaged to daily values.

The groundwater monitoring boreholes (Fig. 1a, Table 3) were located close to Shortandy Lake (GrdW 1) and in Burabay Lake watershed (GrdW 2, 3 and 4). All boreholes are situated at a higher elevation relative to the lakes (Table 3). GrdW 4 is located in the vicinity of the origin of Sary-bulak River (Fig. 1a). Groundwater in this part of BNNP is very fresh (0.07-0.40 g L^{-1}) dominated by bicarbonate and sulphate anions, similarly to Burabay and Shortandy lake water (Dosumov et al., 2014), (see Fig. 1b and Table 1).

3.5. Auxiliary data

Only a few precipitation samples were available for stable isotope analyses in BNNP (see Table 3). The monthly SWI composition of precipitation necessary for IMB modeling was downloaded from waterisotopes.org (Bowen, 2018) using BNNP coordinates and mean elevation (latitude 52.99 °N, longitude 70.22 °E, altitude 300 m). There are no SWI precipitation data available nearby BNNP from the Global Network of Isotopes in Precipitation (GNIP) database (International Atomic Energy Agency, 2015). The closest stations with GNIP records are located in Siberia, ~300 km to the north (Omsk) and 600 km to the north-east (Barabinsk) of BNNP. To define the source water for IMB (e.g. Fellman et al., 2011) the Local Meteoric Water Line (LMWL) obtained at Omsk was used: δ^2 H= 7.47 × δ^{18} O+ 1.7 (see supplementary data in Hughes and Crawford, 2012).

3.6. Water balance, stable isotope mass balance and stable isotope hydrocalculator

Firstly, we applied a long-term lake water balance (WB) method for the hydrological year of 2015–2016 (i.e. from the ice-on of the antecedent year to ice-on of the following year) where we calculated lake water balance for lakes and their watersheds separately (see Yapiyev et al., 2019):

$$\Delta S = P_L + W_y - E_L \tag{11}$$

where ΔS is a change in lake water storage, P_L – precipitation over the lake, W_y – catchment water yield (surface and groundwater inflow to the lake, including the gain from precipitation falling on the catchment land area or the depth-equivalent runoff) and E_L - the lake evaporation. All WB components are in mm of water per year.

Briefly, to obtain annual catchment water yield (Wy) for each lake, we subtracted actual evapotranspiration from catchment (AET) obtained using Budyko curve (see Section 3.5.2 in Yapiyev et al., 2019 for details) from station precipitation (P) then multiplied it by Ratio Catchment/Lake Surface Area (r_{sa}) (see Table 1). Summing P_L and Wy provides Total Inflow, I_L to the lake. The Outflow is annual ice-free E_L for the year 2016 as obtained from the our previous work (Yapiyev et al., 2019). The difference between Total Inflow and Outflow (for BNNP Outflow ≈ E_L) provides an estimate of water storage change for 2016, in this case:

$$\frac{E_L}{I_L} = \frac{E_L}{P_L + W_y} \tag{12}$$

Secondly, we used daily Lake Levels (LL) measurements and annual E_L (see above) to estimate all the water inputs to the lake, I_L, and E_L/I_L. Lake level change (ΔLL) denotes the water storage change as BNNP lakes are endpoints for all water excess in their catchments:

$$\frac{E_L}{I_L} = \frac{E_L}{E_L + \Delta LL} \tag{13}$$

In order to correctly account for all incoming water fluxes to the lakes, we assessed ΔLL from the perspective of a hydrological year. This way we subtracted LL recorded on 1 November 2015 from LL recorded on 31 October 2016 (Kazhydromet measurement at 1 cm precision).

Finally, we calculated IMB using the stable isotope results and the meteorological data using the Hydrocalculator (Skrzypek et al., 2015) software based on a modified Craig-Gordon model. E_L/I_L was estimated based on the initial pool volume value or inflow (defined in Hydrocalculator as δ_P, but here as δ_I), the final stable isotope composition of water in a lake or reservoir (δ_L), precipitation (δ_{rain}), relative humidity and air temperature.

The E_L/I_L ratio and slope of LEL for each lake at the beginning (sampling #1) and the end of open water season (sampling #2) were estimated using measured values, and inputs and monthly precipitation δ^{18}O and δ^2H (mean between April and October) from waterisotopes.org for BNNP (defined in Hydrocalculator as δ_{Rain}). Mean daily relative humidity (decimal fraction) and air temperatures (°C) for sampling campaigns # 1 and #2 from Burabay's weather station (for Kishi Shabakty and Ulken Shabakty Lakes) and AWS Davis (for Shortandy and Burabay Lakes) were used (Fig. 1a). Local data for the source water stable isotope composition, required for the IMB calculations, were not available. Instead, Omsk' LMWL crossing fitted LEL was used (δ^2H =-108.4‰, δ^{18}O = −14.5‰). The steady state model of Hydrocalculator for BNNP lakes was applied with option-3 (isotopic composition of ambient air moisture (δ_a) based on δ_{rain} (δ_P in our case) and adjusted versus LEL). Bennett et al. (2008) proposed adjusting δ_a accounting for its departure from isotopic equilibrium with δ_p due to seasonality effects. Skrzypek et al. (2015) implemented a formulation by Gibson (2014) for adjusting δ_a:

$$\delta_a = (\delta_P - k \times \varepsilon^+)/(1 + k \times \varepsilon^+ \times 10^{-3}) \tag{14}$$

where k is an adjustment parameter ranging from 0.6 to 1 obtained from S_{LEL2} (Eq. 10, see (Skrzypek et al., 2015) for details). Please note, only IMB was calculated for Kishi Shabakty Lake due to the absence of a lake evaporation estimate.

Table 2
The list of key variables with the description and references to sources and equations.

Variables	Description	Equation	Source
δ_I	Isotopic composition of inflow (‰)		assumed
δ_L	Isotopic composition of lake (‰)		measured
T	Air temperature (C°)		measured
δ_a	Isotopic composition of atmospheric moisture (‰)	Eq. 14	Hydrocalculator
k	Adjustment parameter for δ_a		Hydrocalculator
h	Relative humidity (fraction)		measured
δ_P	Isotopic composition of precipitation (‰)		measured
ε^+	Equilibrium isotope separation (‰)		Hydrocalculator
α^+	Equilibrium isotope fractionation (‰)		Hydrocalculator
C_k	Kinetic separation constant (‰)		Hydrocalculator
m	Calculation factor	Eq. 6	Hydrocalculator
ε	Total isotope fractionation factor	Eq. 7	Hydrocalculator
δ^*	Limiting isotope composition enrichment (‰)	Eq. 8	Hydrocalculator
S_{LEL}	Slope of Local Evaporation Line	Eqs. 9 and 10	calculated
τ	Lake water residence time (years)	Eq. 15	calculated
x	Annual throughflow index	Eq. 5	calculated
V_L	Lake volume for 2016 (mm)		(Yapiyev et al., 2019)
d-excess	deuterium excess (‰)	$\delta^2H - 8\delta^{18}O$	calculated
P_L	Precipitation over the lake (mm)		measured
E_L	Lake evaporation (mm)		(Yapiyev et al., 2019)
W_y	Catchment water yield (mm)		calculated
E_L/I_L WB	Evaporation over inflow ratio based on water balance	Eq. 12	calculated
E_L/I_L ΔLL	Evaporation over inflow ratio based on lake levels	Eq. 13	calculated
E_L/I_L IMB	Evaporation over inflow ratio based on isotopic mass balance	Eq. 5	Hydrocalculator

3.7. Residence time

A combination of findings from our previous work on BNNP, where lake volume changes and annual lake evaporation (Yapiyev et al., 2019) were estimated, and new data gathered on SWI composition of the lakes, allowed us to calculate lake water residence time for the year 2016 using:

$$\tau = x\frac{V_L}{E_L}(\text{years}) \tag{15}$$

Where V_L is lake volume (in mm of water layer equivalent), E_L is lake evaporation (in mm of water layer), x is annual throughflow index (isotope based) (Bennett et al., 2008) that equals E_L/I_L in Eq. 5, but δ_L is an arithmetic mean of monthly measurements for the year (see Table 3). The values of x varied between 0 and 1, so when $x = 1$, it is a closed lake system where $E_L = I_L$ (see also Section 2.1 in Gibson et al., 2016 for details). The estimation of water residence allows for determining the sensitivity of lakes to drought. It can also be further used to evaluate susceptibility of lakes to anthropogenic contamination and nutrient loading. Table 2 summarizes the key variables used in this work.

4. Results and discussion

4.1. Stable hydrogen and oxygen isotope compositions

The stable isotope results (δ^{18}O vs. δ^2H) in BNNP (n = 54) formed two distinct clusters (Fig. 2, see also Table 3). The lake water samples form a clearly distinct LEL with δ^{18}O varying between -2.1 and -6.1‰, and δ^2H between -35.4 and -58.5‰. All precipitation data fall close to the expected LMWL. The estimated LMWLs are based on: i) a limited number (4) of collected samples (slope 7.14); ii) precipitation interpolated from global dataset (Bowen et al., 2005) (slope 7.28); and iii) stable isotope precipitation recorded at GNIP Omsk station (slope 7.47), have very similar equations (Fig. 2). The fitted LEL, the regression line for all sampled lakes, crosses LMWLs at δ^{18}O of -15.6 ± 1.1‰ and δ^2H of -115 ± 6.6‰ (Fig. 2), slightly below stream water (-13.2 ± 0.5‰, -97.1 ± 4.1‰) and groundwater values (-13.7 ± 0.4‰, -101.4 ± 2.5‰).

4.2. Stable hydrogen and oxygen isotope composition in precipitation

The results of SWI analyses of collected precipitation samples (n = 5) are close to the expected monthly mean precipitation interpolated from global dataset (Bowen et al., 2005) at BNNP (Fig. 3). As expected, the lowest δ-values for δ^2H and δ^{18}O are found for the winter months (-160 ± 26‰, -21.9 ± 3.7‰), are characterized by low precipitation (7.4–14.2 mm month^{-1}) but have relatively high relative humidity (75–81 %), whereas the highest δ-values are found for the summer months, from May to September (-59.2 ± 7.5‰, -8.0 ± 0.9‰), when precipitation is higher (14–113 mm month^{-1}) but the relative humidity is on average lower

Table 3
Stable isotope composition of water samples from various sources collected between December 2015 and November 2016 in BNNP. The symbol sigma (б) denotes the standard deviation of δ^2H and δ^{18}O.

Sample description	Number of samples, n	Coordinates		Elevation, msl	δ^2H (‰, VSMOW)	б	δ^{18}O (‰ VSMOW)	б	*d-excess*
		lat, N	lon, E						
Precipitation									
rainfall	3	53.129611°	70.279867°	309	−87.8	38.3	−12.1	5.3	8.6
snow	2	52.988853°	70.218467°	390	−143.0	51.9	−19.8	7.2	15.3
Sampled average	5				−115.4	45.1	−15.9	6.3	11.9
Gridded average				300	−105.8		−14.4		9.8
Omsk weighted	8	55.01°	73.38°		−98.8		−13.5		8.9
Groundwater									
GrdW 1	4	52.981149°	70.243706°	433	−100.8	1.7	−13.4	0.4	6.2
GrdW 2	3	53.017697°	70.281484°	391	−99.6	2.6	−13.6	0.4	8.9
GrdW 3	3	53.051782°	70.292704°	347	−99.2	4.9	−13.5	0.7	8.9
GrdW 4	3	53.011514°	70.356100°	385	−106.1	1.0	−14.4	0.1	8.7
Average					−101.4	2.5	−13.7	0.4	8.2
Streams									
Imanai brook	4	53.079097°	70.226137°	344	−97.0	3.1	−13.2	0.3	8.6
Sary-Bulak river	2	53.065006°	70.300079°	308	−97.2	5.0	−13.2	0.6	8.7
Average					−97.1	4.1	−13.2	0.5	8.7
Lakes									
Burabay	8	53.087915°	70.288249°	323	−56.3	1.2	−5.6	0.3	−11.1
Shortandy	8	52.987400°	70.219652°	396	−45.5	0.8	−4.0	0.3	−13.3
Kishi Shabakty	6	53.075871°	70.103341°	306	−46.0	2.4	−4.5	0.4	−9.9
Ulken Shabakty	8	53.127388°	70.277036°	298	−37.4	2.6	−2.7	0.3	−15.7
Average					−46.3	1.8	−4.2	0.3	−12.5
total	54								

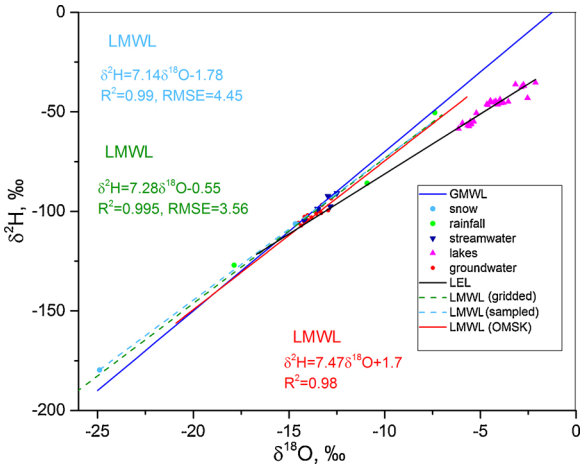

Fig. 2. Stable isotope results of all water samples collected in BNNP (precipitation, lake water, streams, and groundwater). GMWL is in dark blue. LMWLs are based on collected samples (dashed light blue line), interpolated from the global gridded data set (green dashed line; Bowen et al., 2005), or obtained from Omsk GNIP station (red solid line; amount weighted least squares regression method, Hughes and Crawford, 2012). The black solid line is a fitted LEL, i.e., a regression line for all lakes sampled.

(48–76 %) (Fig. 3). Overall, the annual monthly mean δ^2H (−105.8‰) and δ^{18}O (−14.4‰) reflect cold and arid conditions. The total precipitation recorded during the sample collection period, December 2015 – November 2016, was 407 mm (as recorded at 'Burabay' weather station).

The empirical equations (Eq. 16 and 17) that predict δ^2H and δ^{18}O in precipitation as a function of temperature (Dansgaard, 1964; Leibundgut and Maloszewski, 2011) explain well the observed range of variation.

$$\delta^2 H = -5.6T_a - 100(‰) \quad (16)$$

$$\delta^{18} O = -0.69T_a - 13.6(‰) \quad (17)$$

where T_a is the mean annual air temperature in ºC.

Using the mean long-term annual T_a from the Shuchinsk weather station (1.4 °C), Yapiyev et al. (2017b) indicated returns values of −107.8‰ for δ^2H and −14.6‰ for δ^{18}O. These values are in the range of δ-values measured in the collected precipitation

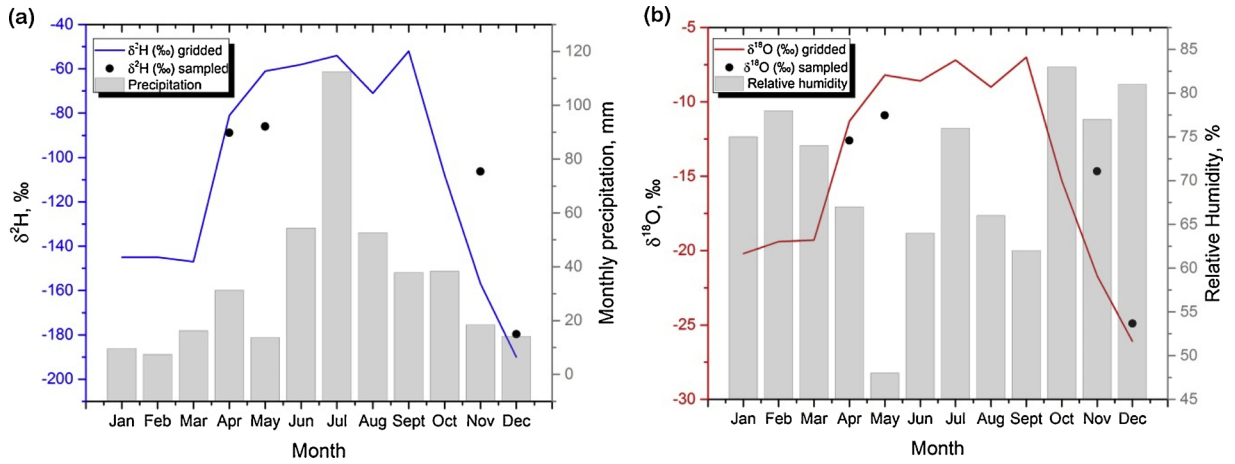

Fig. 3. BNNP SWI values for precipitation as obtained from waterisotopes.org (lines) and measurements made within this study (dots) for (a) δ^2H presented together with monthly precipitation ('Burabay' weather station, 2016) and (b) the equivalent for δ^{18}O, but shown together with monthly relative humidity (obtained from 'Burabay' weather station, 2016). Please note, April measurement point is mean of two samples.

samples, δ^2H -115.44 ± 45.1‰ and δ^{18}O -15.9 ± 6.9‰ (Table 3), and similar to those interpolated from the global dataset δ^2H −105.8‰ and δ^{18}O −14.4‰. The GNIP station at Omsk recorded annual average values in precipitation of −103‰ for δ^2H and −13.9‰ for δ^{18}O (International Atomic Energy Agency, 2015). This comparison suggests that the dataset interpolated for the study site from the global dataset is a good approximation sufficient for calculation of the water inputs.

4.3. Stable hydrogen and oxygen isotope composition in groundwater and streams

The tight clustering of groundwater (n = 13) and stream water (n = 6) results around the GMWL indicates relatively low seasonal and spatial variability in the stable isotope composition inflowing to the lakes in BNNP (Fig. 2). The mean values of δ^2H and δ^{18}O in groundwater samples are -101.4 ± 2.5‰ and −13.7 ± 0.4‰ (Fig. 4, Table 3).

The stable isotope composition of the stream water (δ^2H -97.1 ± 4.1‰ and δ^{18}O −13.2 ± 0.5‰) is very similar to that of groundwater (Fig. 4 and Table 3) with a negligible difference between the two major streams of Imanai Brook and Sary-bulak River discharging into Burabay Lake (Fig. 1). Both stream water and groundwater slightly deviate towards LEL displaying a small evaporative loss (most probably from soil as transpiration is not a fractionating flux), (Fig. 2). Direct and fast interaction between precipitation, stream water and groundwater with minimal evaporative losses prior to recharge results in very close δ-values of these components and well-defined the stable isotope input signal of water discharging to the lakes in the catchments inside of the granite dome of Kokshetau Ridge (Burabay and Shortandy Lakes).

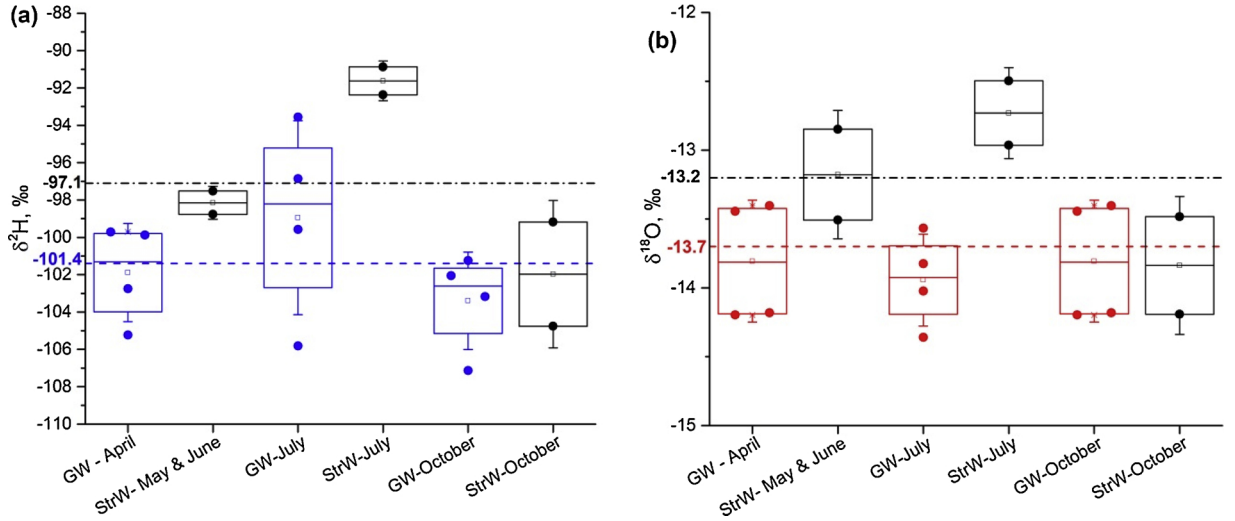

Fig. 4. Seasonal variability of SWI in groundwater (GrdW) and stream water (StrW): δ^2H (a) and δ^{18}O (b). Boxplots: the boxes represent the 25 and 75 percentile; whiskers are 1 standard deviation; actual data points overlap the boxplots; horizontal lines are mean values for all groundwater (δ^2H -blue dash (a), δ^{18}O – red dash (b)) and stream water samples (black dash-dot) with values on y-axis in bold.

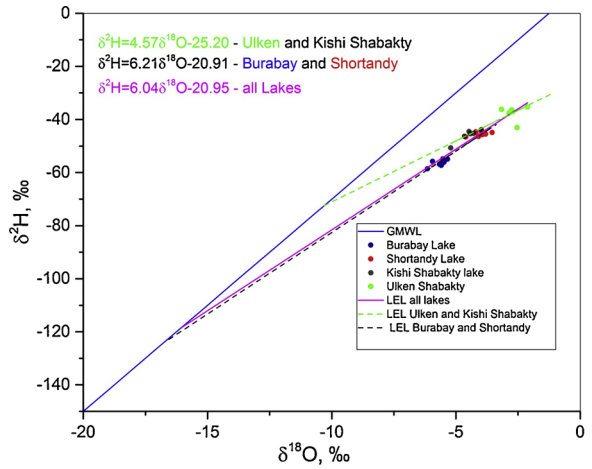

Fig. 5. Stable isotope composition of lake water samples from 2016. The blue line is the GMWL, magenta solid line is fitted LEL (regression line for all lakes sampled), the black dashed line is fitted LEL for Burabay and Shortandy, the green dashed line is fitted LEL for Ulken and Kishi Shabakty, and the dots are individual samples for each lake (blue - Burabay, red –Shortandy, black – Kishi Shabakty, and green – Ulken Shabakty). Also indicated are the regression equations for each LEL type.

Recently Wu et al. (2019) published results of a survey of surface water stable isotope across Kazakhstan. Based on a limited number of rivers samples for Northern Kazakhstan (n = 15), the reported δ^2H varied between -106.2 and −67.5‰ (mean −91.9‰) and δ^{18}O between -10.6 and −13.6‰ (mean −12‰) (Wu et al., 2019). Our data for the stream water are in the range of the reported river samples collected mostly in the same drainage basin (Esil or Ishim River basin).

4.4. Stable isotope composition of lake waters and LEL slopes

The stable isotope composition of lake water samples (n = 30) is characterized by a unique signature for each lake (Figs. 5 and 6, Table 4). The grouping of lake samples on the LEL confirms the highest degree of evaporation enrichment for Ulken Shabakty Lake (i.e. its points are clustered farthest away from the GMWL). The shortest retention time and therefore the lowest evaporative losses are expected for the lakes characterized by the lowest δ-values, suggesting indirectly a possibility for the highest groundwater inflow in Burabay Lake in 2016.

The slope of LEL is primarily driven by relative humidity of air at a given location. Therefore, it also reflects the dynamics of water vapor exchange which may vary depending on the lake size and topography. The individual slopes (S_{LEL}) can be calculated using different methods (Table 4). In general, LEL slopes calculated based on Eq. 9 (S_{LEL1}) are closer to fitted LEL than when these slopes are calculated using Eq.10 (S_{LEL2}). S_{LEL2} can be interpreted as more realistic evaporation slopes, reflecting atmospheric moisture conditions for this part of Northern Central Asia, as opposed to S_{LEL1} for which the results can be biased as a result of GW inputs into lakes. The 'true' long-term evaporation slopes for BNNP and the surrounding region are between 5.2 and 5.7 as reflected in the

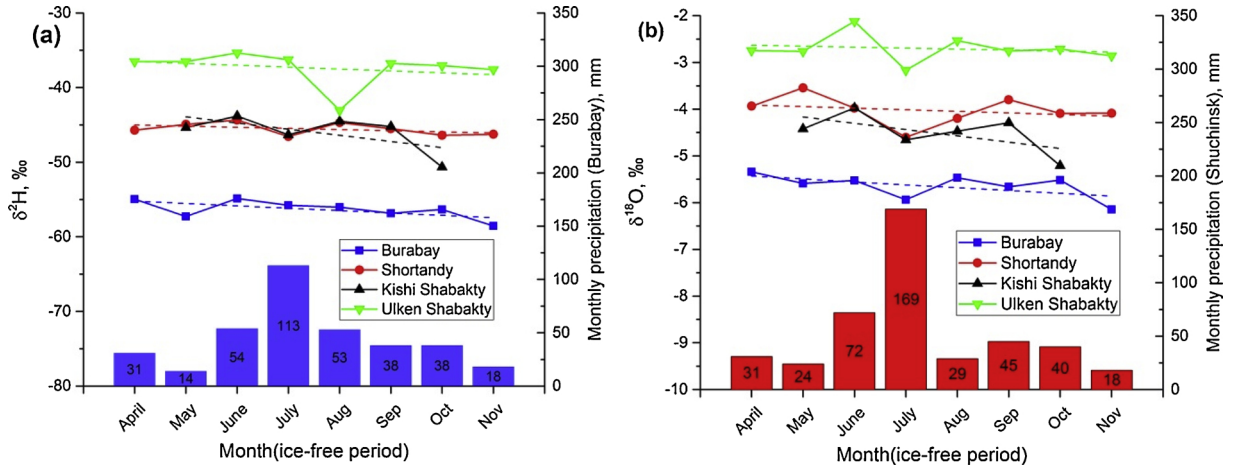

Fig. 6. Seasonal variability in SWI for individual lakes during the ice-free period for δ^2H (a) and δ^{18}O (b). The dashed lines are linear trends for each time-series. The bar plots are monthly precipitation for 'Burabay' (a) and 'Shuchinsk' (b) weather stations where numbers represent monthly precipitation totals (see Fig. 1a for weather station locations).

Table 4
LEL slopes for individual lakes. S_{LEL1} is calculated with adjusted δ_a (see Eq. 14 and related text in the Materials and Methods section).

S_{LEL}	S_{LEL1} Eq. 9	S_{LEL2} Eq. 10	Fitted S_{LEL}
Burabay	6.12	5.34	6.21
Shortandy	6.02	5.34	
Ulken Shabakty	5.17	5.13	4.57
Kishi Shabakty	5.30	5.13	
Average	5.65	5.24	5.39

convergence of arithmetic means of S_{LELs} and fitted slopes (Table 4). This is also in agreement with recent data reported by Wu et al. (2019) with S_{LEL} of 5.66 for lakes in North Kazakhstan (n = 55). The lakes with the highest difference between S_{LEL1} and S_{LEL2} (Burabay and Shortandy) are likely characterized by the largest groundwater input. Based on surveys conducted from 2012 to 2015 in different regions of Kazakhstan Wu et al. (2019) reported S_{LEL} of 6.23 for Kazakh lakes (n = 77); however, this was without consideration of groundwater input. Though this value is close to S_{LEL} for all lake samples from BNNP (Fig. 5) the slope may be too steep to be representative of all Kazakhstani territory which is mostly arid.

The δ^2H and δ^{18}O show a seasonal variation that varies per lake (Fig. 6). The very modest slopes of the linear trend lines are a reflection of the very low cumulative evaporation over summer and relatively constant evaporation over inflow ratios (E_L/I_L) for all lakes (Fig. 6). These results and our previous estimates of lake water volumes and surface water extent changes over the past 30 years (Yapiyev et al., 2019) confirm that BNNP lakes are generally in a steady-state. The close resemblance of isotopic 'signatures' between Shortandy and Kishi Shabakty lakes was unexpected because these lakes have very different hydrological and limnologic characteristics (Table 1, Fig. 1), (Yapiyev et al., 2017b). We hypothesize that this match can be due to similar long-term E_L/I_L values and water residence times. Kishi Shabakty Lake' catchment surface area is about two times larger than Shortandy's, but its water volume is almost 40 % smaller (see Table 1). Thus Kishi Shabakty Lake has a larger watershed water yield than Shortandy Lake, but higher evaporation losses which are similar to those calculated for Ulken Shabakty (see Table 5).

Mizota et al. (2009) reported δ^{18}O values from a single sampling campaign from several lakes across northern Kazakhstan. For example, the δ^{18}O value from a saline shallow steppe Lake Teke (-4.4‰) located around 200 km to north-east from BNNP was identical to the mean of δ^{18}O (−4.4‰) for all BNNP lake water samples (see Table 3). The other locations: Lake Tengiz (~ 300 km to the south-west from BNNP) and Kushmurun Lake (~ 400 km to the west from BNNP) had much higher δ^{18}O values of −0.9 and −1.2‰ respectively. This indicates that most probably BNNP lakes have E_L/I_L regime more similar to the closed lakes in the southern part of Siberia than to the steppe lakes located in more arid parts of Central Asia.

4.5. d-excess

Mean d-excess for precipitation from the gridded data (9.78‰) and sample data (11.9‰) (Table 3) are close to the global average of 10‰ (Brooks et al., 2014). Moreover, *d-excess* values for groundwater (8.2‰) and streams (8.7‰) were close to *d-excess* values for weighted precipitation at Omsk (8.9‰) (see Table 3 and Fig. 7a). This observation serves as an additional confirmation for the validity of the use of Omsk's LMWL for source water determination in our IMB calculations. In sharp contrast, the *d-excess* values for the lakes are very low, ranging from -8.6‰ for Kishi Shabakty Lake to -15.7‰ for Ulken Shabakty Lake (Table 3, Fig. 7b). The most negative *d-excess* in lake water of Ulken Shabakty indicates not only a high degree of evaporation but also the prevalence of 'old'

Table 5
Estimation of the water balance of three BNNP lakes for 2016 by three methods (WB, IMB and LL) see Materials and Methods).

Lake	Ulken Shabakty	Burabay	Shortandy
Precipitation, P (mm/year)	409	508	508
Lake Evaporation, E_L (mm/year)	631[1]	643[1]	502[1]
Catchment AET (mm/year)	359	419	419
Ratio Watershed/Lake Area, r_{sa}	8.15(3.15)*	16.4	4.76
Water Yield, Wy (mm/year)**	408 (158)*	1460	424
Total Inflow, $P_L + W_y$ (mm/year)	817	1968	932
Change in Lake Storage, ΔS (mm/year)	186	1325	430
E_L/I_L, WB[1]	0.77(1.11)*	0.33	0.54
E_L/I_L, Δ LL	0.71	1.05	0.80
E_L/I_L, IMB***	0.69	0.34	0.53
E/I difference, Δ LL- IMB	0.02	0.71	0.27
Ratio Water Yield/Total Inflow, (%)	49.9	74.2	45.5

[1] see (Yapiyev et al., 2019), *this r_{SA} is based on reduced watershed area/lake area ratio, ** $W_y = r_{SA}(P - AET)$ the water depth-equivalent runoff to a lake (see also section 3.7), *** based on mean of δ^2H and δ^{18}O. Note, Kishi Shabakty Lake is not represented in this table due to the absence of a lake evaporation estimates and lake level observations. Mean IMB E_L/I_L for Kishi Shabakty is 0.46 (see also Fig. 8).

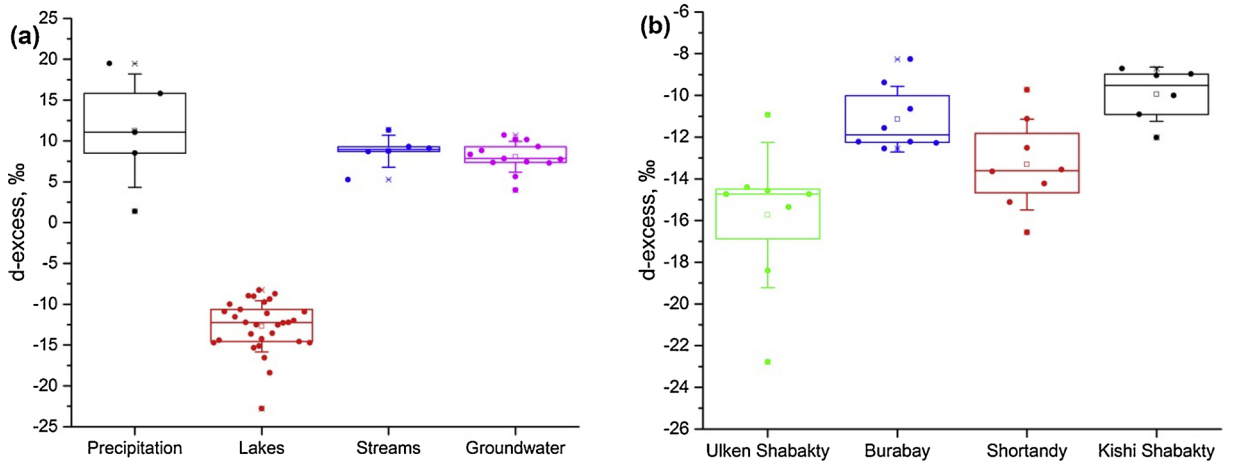

Fig. 7. Boxplots of d-excess in (a) precipitation (sampled), lakes, streams, and groundwater; (b) individual lakes. Boxplots: the boxes are 25 and 75 percentile, whiskers are 1 standard deviation, and actual data points overlap the boxplots.

evaporated water, as well as low inputs from snowmelt/groundwater into its basin.

4.6. Water and stable isotope mass balance – water lake residence time

The water balance for three lakes has been calculated using three different methods to verify each method and obtain the most accurate results possible (Table 5 and Fig. 8). Kishi Shabakty Lake's level and surface water temperature were not monitored by Kazhydromet, therefore, its water balance is estimated only by the IMB method (Fig. 8, see also Table 5 footnote). Additionally, watershed inflow (yield) as a fraction of the overall water balance ($W_y/P_L + W_y$, expressed as a percentage) was calculated to characterize the degree of groundwater-dependence of the lakes (see Table 5 bottom row). Water Budget (WB, see Eq. 12) and stable Isotope Mass Balance (IMB) methods (Eq. 5) provided very similar E_L/I_L ratios for all the lakes. However, the water budget estimate by Lake Level change (ΔLL, see Eq. 13) is in good agreement with IMB only for Ulken Shabakty Lake (based on full watershed area/lake area ratio, see Table 5 footnote). For Burabay and Shortandy, there is a significant difference (see Table 5, and Fig. 8).

In 2016 the water balance of Ulken Shabakty Lake was positive for the first time since 2008 as its water level rose by 27 cm since the end of October 2015. The previous estimates of the long-term water balance of this lake showed that its *Wy* is substantially reduced as a result of the isolation of a large part of the watershed to the south-east of the lake and due to road construction and Burabay settlement developments (see Fig. 1a) (Yapiyev et al., 2019). However, WB estimate for Ulken Shabakty for 2016 based on full watershed area r_{sa} (8.15) corresponds much better to the other two water budget methods results (IMB and ΔLL). Ulken Shabakty occupies the lowest position in the landscape among the three lakes (with the order from highest to lowest being Shortandy-Burabay-Ulken Shabakty, Fig. 1b), and excess water in the lakes system inside of Kokshetau ridge is "spilled" downgradient (mostly by subsurface flow) into Ulken Shabakty which could be considered a terminal lake with limited outflow. The outflow of excess water from Shortandy and Burabay to Ulken during wet years, rather than losses in the form of evaporation, is confirmed by the lack of a trend in increasing $\delta^{18}O$ (see Fig. 6a). Thus, isotopic evaporative signatures match with E_L/I_L by the WB and ΔLL methods for Ulken Shabakty, but there is a discrepancy for Burabay and Shortandy. From 1 November 2013 to 31 October 2016, the LL increased by 27 cm and 13 cm for Ulken Shabakty and Shortandy, respectively, and decreased by 3 cm during this period for Burabay. These changes

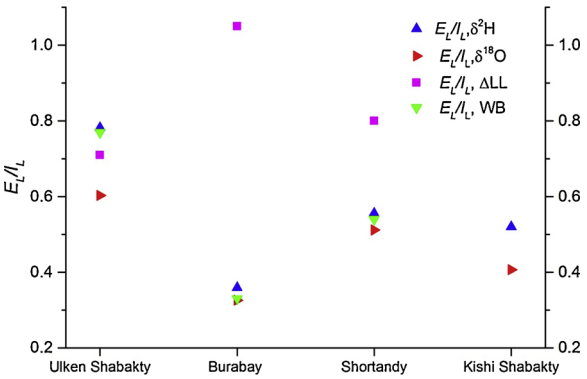

Fig. 8. E_L/I_L for four BNNP Lakes for the year 2016 by catchment water balance method, based on LL and annual evaporation, and δ^2H and δ^{18}O (see methods section).

in LL determine E_L/I_L values for the lakes (Table 5): < 1 (positive water balance or gain in storage) for Ulken and Shortandy, and > 1 for Burabay (negative water storage, more evaporation than inflow). Moreover, IMB almost perfectly fits the independent catchment WB estimates for Shortandy and Burabay (E_L/I_L ratios differences are within ± 0.01). We propose that this difference between ΔLL and IMB E_L/I_L ratios for Burabay and Shortandy lakes is due to non-evaporative loss (subsurface flow) of water towards Ulken Shabakty's basin. To confirm this hypothesis and calculate the 'missing' volume, we subtracted IMB's E_L/I_L from ratios based on lake level change (ΔLL) for Shortandy and Burabay (see Table 5 second row from bottom). Next, for each lake, this excess water (131 and 456 mm for Shortandy and Burabay) was multiplied by the lake evaporation in mm (see Table 5) and then multiplied by each lake surface area in m^2 in order to obtain the amount of water volume in litres. Finally, we calculated this water volume for Burabay and Shortandy and divided it by Ulken Shabakty's lake area to calculate the equivalent of this excess in mm of water layer as received by Ulken's Shabakty Lake. The final figure of 359 mm water fits reasonably well with the 270 mm rise in LL of Ulken Shabakty for the hydrological year. The water excess in Burabay Lake (456 mm) is equivalent to a water layer of 253 mm depth over Ulken Shabakty Lake' total lake area. This likely suggests that the adjacent Burabay Lake and its watershed contributed considerably to the substantial water level rise of Ulken Shabakty in 2016.

BNNP is dominated by fractured rocks (Fig. 1b), resulting in high permeability of the subsurface zone. Yapiyev et al. (2017b) provide evidence of very good connectivity between the aquifer and the lake. Our assumption is that the watershed inflow at BNNP is mediated by groundwater. This assumption is also confirmed by stable isotope data and it applies in particular to Shortandy Lake which has no surface inflow/outflows (Fig. 4). In 2016, watershed inflow ranged from 45.5 % for Shortandy and 50 % for Ulken Shabakty Lakes to 74 % for Burabay Lake (Table 5). Our long-term (1986–2016) water balance estimates of BNNP lakes (Yapiyev et al., 2019) indicate that the watershed inflow ranges from about 31 and 12 % (based on reduced watershed area) for Shortandy and Ulken Shabakty Lakes, respectively, to 61 % for Burabay Lake (data not shown). Watershed inflow for Ulken Shabakty based on full watershed area is about 44 % and should result in a positive water balance (increase in lake water level), but this contradicts the observed long-term water balance and lake level changes (Yapiyev et al., 2019). Under current conditions, the water balance of Ulken Shabakty can be positive only after a succession of very wet years, as was also observed in the recent period (after 2015).

Burabay Lake has the shortest residence time among the four lakes with its V_L/E_L ratio indicating that around 20 % of its volume is lost through evaporation (Table 6). Shortandy and Ulken Shabakty have the longest water residence times as their volumes are more than five times larger than that of Burabay (Table 1). Shortandy is the most balanced among the lakes with the largest volume and lowest evaporation thus yielding the highest V_L/E_L ratio (Table 6, see also Yapiyev et al., 2019). Though Burabay Lake water levels have been the most stable in the long-term, this lake depends heavily on its large watershed inflow and its volume can quickly decline in dry years with extremely low precipitation. Despite the fact that Ulken Shabakty is experiencing a long-term water level decline (Yapiyev et al., 2017b), it remains a relatively large lake as indicated by substantial V_L/E_L ratio and water residence times (Table 6). Water levels for this lake slightly recovered due to a succession of wet water years (2013–2016), but E_L continues to rise even in wet years and this is most probably due to the advection of hot dry air during summer from the steppe to the north (Yapiyev et al., 2019). The calculated water residence times in the lakes also suggest that Burabay can be highly susceptible to contamination by watershed runoff from its large catchment.

4.7. General discussion

Surface and groundwater watershed divides may not necessarily overlap in complex geological terrains (Winter et al., 2003). Tromp-van Meerveld and McDonnell (2006) proposed the 'fill and spill' hypothesis to explain subsurface stormflow run-off generation on hillslopes following the filling of macropores on the soil-bedrock interface and water transfer between different watersheds. They linked this significant subsurface shallow run-off generation with a threshold precipitation event when water in saturated areas becomes connected to a trench on a hillslope. Winter and Carr (1980) demonstrated that in North Dakota local groundwater flow system discharges water to topographical lows, while upper wetlands seem to recharge groundwater. Shaw et al. (2012) examined 'fill and spill' events in Canadian Prairie wetland complexes and concluded that the watershed contributing area to an outlet and run-off generation have a dynamic and intermittent nature. Such events can cause sudden rises of water level in the terminal basins depending on antecedent watershed conditions. The assumption on reduced watershed area is correct for most of the regular years for Ulken. The WB estimate for Ulken Shabakty for 2016 based on the entire watershed area, r_{SA} (E_L/I_L = 0.77) corresponds much better to the other two water budget methods results based on IMB (0.69) and lake levels (0.71), than the one based on the reduced watershed. This can be explained by the occurrence of overflow of water from Burabay and Shortandy's watersheds to Ulken Lake. It may also suggest that sharp and significant increases in precipitation enhanced hydraulic connectivity in Ulken's watershed in 2016. The exact size of the watershed area contributing to run-off to Ulken in 2016 is not known; its determination would require

Table 6
Water residence time for three BNNP lakes in 2016.

Lake	V_L/E_L*	annual throughflow index, (x)**	Residence time, years (τ)
Ulken Shabakty	14.6	0.7	10.2
Burabay	4.9	0.38	1.9
Shortandy	24.3	0.54	13.1

*Water residence times based on V_L and E_L for 2016 (see Yapiyev et al., 2019), ** x equals E_L/I_L (see Materials and Methods section).

more data, such as a high-resolution (1 m or higher) Digital Elevation Model (DEM) which was not available for this study.

BNNP experienced three drought years: 2008, 2010 and 2012, with low P (208, 258 and 314 mm year^{-1}, Shuchinsk) and high PET (838, 911 and 904 mm year^{-1}) when lake levels substantially decreased by 0.8–1.5 m (Yapiyev et al., 2019, 2017b). These years were characterized by high E_L ranging from 528 to 718 mm year^{-1} (Yapiyev et al., 2019). Starting from 2013, the precipitation increased and by 2016 was characterized as the second largest total annual precipitation record (523 mm year^{-1}) for the period from 1935 to 2016 (Shuchinsk weather station, see Fig. 1a). This succession of wet years led to 'filling' of Shortandy and Burabay Lake watersheds and 'spilling' into Ulken Shabakty Lake in 2016. Almost 50 years ago, a similar water level rise was recorded and described by Soviet hydrogeologists for Ulken Shabakty Lake (called Bolshoe Chebachie at that time, this name is still in use) (Zemlyanitsina, 1970). From 1958–1961 Ulken Shabakty water level rose by approximately 2 m, preceded by a ten year (1948–1958) water level decline of more than 2.5 m due to drought conditions (Uryvaev, 1959; Zemlyanitsina, 1970). Note that the highest total annual precipitation to date (607 mm year^{-1}) at BNNP was recorded at Shuchinsk weather station in 1960 (Yapiyev et al., 2017b). Interestingly, Zhang et al. (2017) investigated the trends in extreme precipitation in Central Asia from 1938 to 2005. The work was based on an analysis of daily station data, and they identified abrupt changes (increases) around 1957 and 1986. Overall, the year of 2016 had a historical maximum of precipitation (392 mm year^{-1}) across Kazakhstan for the observation period of 1936–2016 (Ministry of Energy, 2017). The water levels of the lakes in the BNNP have been rising since the last drought in 2012. During our last fieldtrip to BNNP in October 2018, it was observed that Ulken Shabakty Lake had continued to rise. Its water level had increased by about 32 cm since October 2016 while Shortandy Lake levels remained unchanged; Burabay rose by approximately 19 cm (Kazhydromet, 2017). This suggests that the lateral groundwater movement from the elevated Shortandy and Burabay Lakes to Ulken Shabakty Lake can take more than a year.

This increase of lake water level coincides with a concurrent rise in water levels observed in the Great Lakes of North America (Gronewold et al., 2016; Gronewold and Rood, 2018; Yapiyev et al., 2017b). Lately, Gronewold and Rood (2018) reported that Lake Ontario that occupies a lowest position and the last in the Laurentian Great Lakes chain rose a record high level in May 2017. Gronewold and Rood (2018) attribute the latest trend of continuing water level rise in the Great Lakes to increased precipitation in the region powered by extreme precipitation events linking those to Arctic amplification (Francis and Vavrus, 2012). They argue that contrary to a common perception that the Great Lakes water levels are regulated by human water management in their basins, the main drivers behind these water storage fluctuations have climatic nature (Gronewold and Rood, 2018). Undoubtable, the Great Lakes are different from BNNP, but there are some similarities with the Earth's largest lake system and the other terminal lakes in the North America (particularly Canadian prairies), such as precipitation, evaporation rates, climate (as both are located approximately on the same latitude) (Van Der Kamp et al., 2008; Yapiyev et al., 2017b). Though BNNP lakes are much more inland, their climate is more continental (Yapiyev et al., 2017b). The present and previous (Yapiyev et al., 2019, 2017b) works on BNNP Lakes demonstrated that its hydrological cycle is regulated primarily by climate variability (change) rather than a direct anthropogenic influences such as water abstraction in its basins.

5. Conclusions

Burabay National Nature Park (BNNP) is an ecotone between boreal forests with humid air and alpine lakes, and arid steppe with a much drier atmosphere. BNNP represents a unique hydrometeorological transition zone between wider Northern Eurasia (including Boreal Siberia) and more arid Central Asia. Though evaporation loss dominates the water cycle at BNNP leading to a long-term decline trend in lake water storage (Yapiyev et al., 2019, 2017b), the groundwater plays an important role particularly in the forested areas dominated by fractured granites. BNNP lake water storage has been replenished recently for the first time in the last 9 years because of unusually high precipitation from 2013 to 2016.

The stable isotope study confirmed that the water balance for Burabay and Shortandy lakes, that are found at higher elevation in forested areas, is more similar to that of lakes found at higher latitudes (e.g., in South Siberia), while those for Kishi and Ulken Shabakty lakes (at lower elevation, and surrounded by steppe) are closer to what has been recorded for the steppe lakes of Central Asia. Ulken Shabakty Lake is a terminal basin in this endorheic lake system and a good proxy of overall hydroclimatic conditions at BNNP. The recent water level rise in Ulken Shabakty Lake observed in 2016 can be explained by a 'fill and spill' mechanism described before on hillslope scale and for boreal wetlands areas. The water stable isotope mass balance and traditional water balance calculations produced very similar results for the annual time scales, confirming that the stable isotope methods are a good proxy for laborious and time-consuming full-scale water budget calculations. The stable isotope model could be further improved by better quantification of inputs from snowmelt, more precise GNIP observations at the study site and direct air moisture stable isotope analyses.

Author contributions

V.Y. conceived and planned the work, collected and processed the samples and observational data, conducted data analysis, wrote and edited the paper. G.S. supervised isotopic modelling and analysis. Z.S. and V.Y. prepared the map. G.S., A.V., Z.S., D.M. helped with data-interpretation, contributed to the text and edited the paper. The authors' names are provided in the order of contribution.

Declaration of Competing Interest

The authors declare no conflict of interest.

Acknowledgments

Funding: This research was supported under the target program No. 0115RK03041 “Research and development in the fields of energy efficiency and energy saving, renewable energy sources, and environmental protection for years 2014–2016” from the Ministry of Education and Science of the Republic of Kazakhstan. We also would like to acknowledge the support from the project, “Climate Change, Water Resources and Food Security in Kazakhstan” (CCKAZ) funded by the United Kingdom’s Newton Fund Institutional Links Programme (Grant No. 172722855). This research was also partially supported under the target program No. BR05236529 “Complex ecosystem assessment of Shuchinsk-Borovoye resort area through the environmental pressure evaluation for the purposes of sustainable use of recreational potential” from the Ministry of Education and Science of the Republic of Kazakhstan. This work was funded by the UK Global Challenges Research Fund (GCRF) "Solutions to secure clean water in the glacier-fed catchments of Central Asia – what happens after the ice?". This research was also supported by Nazarbayev University and Nazarbayev University Research and Innovation System. We are very grateful to Professor Jeffrey McDonnell and Dr. Kim Janzen for sample analysis and constructive comments on the initial version of the manuscript. We also would like to thank engineer Vladimir Novokhatskiy for assistance in installation and maintenance of the equipment. We thank Kazhydromet’s staff at the weather station near Ulken Shabakty Lake for the collection of the precipitation samples. David Macdonald publishes with the permission of the Executive Director, British Geological Survey. The presented work is a part of the lead author’s Ph.D. thesis completed at Nazarbayev University.

Appendix A. Supplementary data

Supplementary material related to this article can be found, in the online version, at doi:https://doi.org/10.1016/j.ejrh.2019.100644.

References

Ala-aho, P., Rossi, P.M., Kløve, B., 2013. Interaction of esker groundwater with headwater lakes and streams. J. Hydrol. 500, 144–156. https://doi.org/10.1016/J.JHYDROL.2013.07.014.

Bennett, K.E., Gibson, J.J., McEachern, P.M., 2008. Water-yield estimates for critical loadings assessment: comparisons of gauging methods versus an isotopic approach. Can. J. Fish. Aquat. Sci. 65, 83–99. https://doi.org/10.1139/f07-155.

Bowen, G.J., 2018. WaterIsotopes.org, Version OIPC3.1 [WWW Document]. URL http://wateriso.utah.edu/waterisotopes/pages/data_access/oipc.html (Accessed 1.19.18). .

Bowen, G.J., Wassenaar, L.I., Hobson, K.A., 2005. Global application of stable hydrogen and oxygen isotopes to wildlife forensics. Oecologia 143, 337–348.

Boyle, D.R., 1994. Design of a seepage meter for measuring groundwater fluxes in the nonlittoral zones of lakes-Evaluation in a boreal forest lake. Limnol. Oceanogr. 39, 670–681. https://doi.org/10.4319/lo.1994.39.3.0670.

Brooks, J.R., Gibson, J.J., Birks, S.J., Weber, M.H., Rodecap, K.D., Stoddard, J.L., 2014. Stable isotope estimates of evaporation : inflow and water residence time for lakes across the United States as a tool for national lake water quality assessments. Limnol. Oceanogr. 59, 2150–2165. https://doi.org/10.4319/lo.2014.59.6.2150.

Craig, H., Gordon, L., 1965. Deuterium and oxygen 18 variations in the ocean and the marine atmosphere. Stable Isot. Oceanogr. Stud. Paleotemp. 9–130.

Dansgaard, W., 1964. Stable isotopes in precipitation. Tellus 16, 436–468. https://doi.org/10.3402/tellusa.v16i4.8993.

Dosumov, A., Deineka, V., Isin, K., Ashimov, A., Kim, D., Timeyeva, L., 2014. Compilation of Modern Hydrogeological Map with Scale of 1:200000 and Map-frames Withscale of 1:50000 of the Territory of Schuchinsk-burabay Resort Area in Akmolaprovince. In Russian. .

Fellman, J.B., Dogramaci, S., Skrzypek, G., Dodson, W., Grierson, P.F., 2011. Hydrologic control of dissolved organic matter biogeochemistry in pools of a subtropical dryland river. Water Resour. Res. 47, 1–13. https://doi.org/10.1029/2010WR010275.

Finch, J., Calver, A., 2008. Methods for the Quantification of Evaporation from Lakes. Report 47.

Francis, J.A., Vavrus, S.J., 2012. Evidence linking Arctic amplification to extreme weather in mid-latitudes. Geophys. Res. Lett. 39https://doi.org/10.1029/2012GL051000. n/a-n/a.

Gat, J.R., 1998. Oxygen and Hydrogen Isotopes in the Hydrologic Cycle 1–38. https://doi.org/10.1146/annurev.earth.24.1.225.

Gat, J.R., 1995. Stable isotopes of fresh and saline Lakes. In: Lerman, A., Imboden, D.M., Gat, J.R. (Eds.), Physics and Chemistry of Lakes. Springer, Berlin Heidelberg, Berlin, Heidelberg, pp. 139–163. https://doi.org/10.1016/0016-7037(96)83277-7.

Gibson, J.J., Birks, S.J., Edwards, T.W.D., 2008. Global prediction of δA and δ2H- δ18O evaporation slopes for lakes and soil water accounting for seasonality. Global Biogeochem. Cycles 22https://doi.org/10.1029/2007GB002997. n/a-n/a.

Gibson, J.J., Birks, S.J., Jeffries, D., Yi, Y., 2017. Regional trends in evaporation loss and water yield based on stable isotope mass balance of lakes: the Ontario Precambrian Shield surveys. J. Hydrol. 544, 500–510. https://doi.org/10.1016/j.jhydrol.2016.11.016.

Gibson, J.J., Birks, S.J., Yi, Y., 2016. Stable isotope mass balance of lakes: a contemporary perspective. Quat. Sci. Rev. 131, 316–328. https://doi.org/10.1016/j.quascirev.2015.04.013.

Gibson, J.J., Reid, R., 2014. Water balance along a chain of tundra lakes: a 20-year isotopic perspective. J. Hydrol. 519, 2148–2164. https://doi.org/10.1016/J.JHYDROL.2014.10.011.

Gonfiantini, R., 1986. Environmental isotopes in lake studies. Handbook of Environmental Isotope Geochemistry; The Terrestrial Environment. Elsevier, pp. 113–168.

Gronewold, A.D., Bruxer, J., Durnford, D., Smith, J.P., Clites, A.H., Seglenieks, F., Qian, S.S., Hunter, T.S., Fortin, V., 2016. Hydrological drivers of record-setting water level rise on Earth’s largest lake system. Water Resour. Res. 52, 4026–4042. https://doi.org/10.1002/2015WR018209.

Gronewold, A.D., Rood, R.B., 2018. Recent water level changes across Earth’s largest lake system and implications for future variability. J. Great Lakes Res. 10–12. https://doi.org/10.1016/j.jglr.2018.10.012.

Horita, J., Rozanski, K., Cohen, S., 2008. Isotope effects in the evaporation of water: a status report of the Craig–gordon model. Isotopes Environ. Health Stud. 44, 23–49. https://doi.org/10.1080/10256010801887174.

Horita, J., Wesolowski, D.J., 1994. Liquid-vapor fractionation of oxygen and hydrogen isotopes of water from the freezing to the critical temperature. Geochim. Cosmochim. Acta 58, 3425–3437. https://doi.org/10.1016/0016-7037(94)90096-5.

Hughes, C.E., Crawford, J., 2012. A new precipitation weighted method for determining the meteoric water line for hydrological applications demonstrated using Australian and global GNIP data. J. Hydrol. 464–465, 344–351. https://doi.org/10.1016/j.jhydrol.2012.07.029.

International Atomic Energy Agency, 2015. Water Isotope System for Data Analysis, Visualization and Electronic Retrieval [WWW Document]. URL. http://www-naweb.iaea.org/napc/ih/IHS_resources_isohis.html.

Kazhydromet, 2017. National Hydrometeorological Service of Kazakhstan [WWW Document]. URL https://kazhydromet.kz/en/p/o-nacionalnoj-

gidrometeorologiceskoj-sluzbe-kazahstana (Accessed 11.7.17). .
Krabbenhoft, D.P., Bowser, C.J., Kendall, C., Gat, J.R., 1994. Use of Oxygen-18 and Deuterium to Assess the Hydrology of Groundwater-Lake Systems. pp. 67–90. https://doi.org/10.1021/ba-1994-0237.ch003.
Leibundgut, C., Maloszewski, P., 2011. Tracers in Hydrology. John Wiley & Sons.
Ma, L., Jilili, A., Li, Y., 2018. Spatial differentiation in stable isotope compositions of surface waters and its environmental significance in the Issyk-Kul Lake region of Central Asia. J. Sci. 15, 254–263. https://doi.org/10.1007/s11629-017-4499-4.
McJannet, D., Hawdon, A., Van Niel, T., Boadle, D., Baker, B., Trefry, M., Rea, I., 2017. Measurements of evaporation from a mine void lake and testing of modelling approaches. J. Hydrol. 555, 631–647. https://doi.org/10.1016/j.jhydrol.2017.10.064.
McMahon, T.A., Peel, M.C., Lowe, L., Srikanthan, R., McVicar, T.R., 2013. Estimating actual, potential, reference crop and pan evaporation using standard meteorological data: a pragmatic synthesis. Hydrol. Earth Syst. Sci. Discuss. 17, 1331–1363. https://doi.org/10.5194/hess-17-1331-2013.
Micklin, P., 2016. The future Aral Sea: hope and despair. Environ. Earth Sci. 75, 844. https://doi.org/10.1007/s12665-016-5614-5.
Ministry of Energy, K, 2017. Annual Monitoring of State of Climate in Kazakhstan: 2016. http://www, January, 2017. .
Mizota, C., Doi, H., Kikuchi, E., Shikano, S., Kakegawa, T., Yurlova, N., Yurlov, A.K., 2009. Stable isotope characterization of fluids from the Lake Chany complex, western Siberia, Russian Federation. Appl. Geochem. 24, 319–327. https://doi.org/10.1016/j.apgeochem.2008.10.009.
Numaguti, A., 1999. Origin and recycling processes of precipitating water over the Eurasian continent: experiments using an atmospheric general circulation model. J. Geophys. Res. D Atmos. 104, 1957–1972. https://doi.org/10.1029/1998JD200026.
Oberhänsli, H., Weise, S.M., Stanichny, S., 2009. Oxygen and hydrogen isotopic water characteristics of the Aral Sea, Central Asia. J. Mar. Syst. 76, 310–321. https://doi.org/10.1016/j.jmarsys.2008.03.019.
Pekel, J.-F., Cottam, A., Gorelick, N., Belward, A.S., 2016. High-resolution mapping of global surface water and its long-term changes. Nature 1–19. https://doi.org/10.1038/nature20584.
Shaw, D.A., Vanderkamp, G., Conly, F.M., Pietroniro, A., Martz, L., 2012. The fill-spill hydrology of prairie wetland complexes during drought and deluge. Hydrol. Process. 26, 3147–3156. https://doi.org/10.1002/hyp.8390.
Shaw, G.D., White, E.S., Gammons, C.H., 2013. Characterizing groundwater–lake interactions and its impact on lake water quality. J. Hydrol. 492, 69–78. https://doi.org/10.1016/j.jhydrol.2013.04.018.
Skrzypek, G., Mydłowski, A., Dogramaci, S., Hedley, P., Gibson, J.J., Grierson, P.F., 2015. Estimation of evaporative loss based on the stable isotope composition of water using Hydrocalculator. J. Hydrol. 523, 781–789. https://doi.org/10.1016/j.jhydrol.2015.02.010.
Sun, C., Shen, Y., Chen, Y., Chen, W., Liu, W., Zhang, Y., 2017. Quantitative evaluation of the rainfall influence on streamflow in an inland mountainous river basin within Central Asia. Hydrol. Sci. J. 1–14. https://doi.org/10.1080/02626667.2017.1390314.
Tromp-van Meerveld, H.J., McDonnell, J.J., 2006. Threshold relations in subsurface stormflow: 2. The fill and spill hypothesis. Water Resour. Res. 42, 1–11. https://doi.org/10.1029/2004WR003800.
Uryvaev, V., 1959. Surface Water Resources of Virgin and Fallow Lands Development Regions Kokshetau Province of KazakhSSR. (In Russian), Surface Water Resources of Virgin and Fallow Lands Development Regions. Hydrometeorological press, Leningrad.
Van Der Kamp, G., Keir, D., Evans, M.S., 2008. Long-term water level changes in closed-basin lakes of the Canadian prairies. Can. Water Resour. J. 33, 23–38.
Wang, S., Zhang, M., Che, Y., Chen, F., Qiang, F., 2016. Contribution of recycled moisture to precipitation in oases of arid central Asia: a stable isotope approach. Water Resour. Res. 52, 3246–3257. https://doi.org/10.1002/2015WR018135.
Winter, T.C., Carr, M.R., 1980. Hydrologic setting of wetlands in the Cottonwood Lake area, Stutsman County, North Dakota. US Geol. Surv. Water Resour. Div. Water Resour. Investig. 99.
Winter, T.C., Rosenberry, D.O., LaBaugh, J.W., 2003. Where does the ground water in small watersheds come from? Ground Water 41, 989–1000. https://doi.org/10.1111/j.1745-6584.2003.tb02440.x.
Wu, H., Wu, J., Song, F., Abuduwaili, J., Saparov, A.S., Chen, X., Shen, B., 2019. Spatial distribution and controlling factors of surface water stable isotope values (δ18O and δ2H) across Kazakhstan, Central Asia. Sci. Total Environ. 678, 53–61. https://doi.org/10.1016/J.SCITOTENV.2019.03.389.
Xiao, K., Griffis, T.J., Baker, J.M., Bolstad, P.V., Erickson, M.D., Lee, X., Wood, J.D., Hu, C., Nieber, J.L., 2018. Evaporation from a temperate closed-basin lake and its impact on present, past, and future water level. J. Hydrol. 561, 59–75. https://doi.org/10.1016/j.jhydrol.2018.03.059.
Yapiyev, V., Sagintayev, Z., Inglezakis, V.V.J.V., Samarkhanov, K., Verhoef, A., 2017a. Essentials of endorheic basins and lakes: a review in the context of current and future water resource management and mitigation activities in central asia. Water 2017 9 (798), 9. https://doi.org/10.3390/W9100798.
Yapiyev, V., Sagintayev, Z., Verhoef, A., Kassymbekova, A., Baigaliyeva, M., Zhumabayev, D., Malgazhdar, D., Abudanash, D., Ongdas, N., Jumassultanova, S., 2017b. The changing water cycle: burabay national nature park, Northern Kazakhstan. Wiley Interdiscip. Rev. Water 4, e1227. https://doi.org/10.1002/wat2.1227.
Yapiyev, V., Samarkhanov, K., Tulegenova, N., Jumassultanova, S., Verhoef, A., Saidaliyeva, Z., Umirov, N., Sagintayev, Z., Namazbayeva, A., Zhumabayev, D., Tulegenova, N., Jumassultanova, S., Umirov, N., Sagintayev, Z., Verhoef, A., Namazbayeva, A., 2019. Estimation of water storage changes in small endorheic lakes in Northern Kazakhstan. J. Arid Environ. 160, 42–55. https://doi.org/10.1016/j.jaridenv.2018.09.008.
Yi, Y., Brock, B.E., Falcone, M.D., Wolfe, B.B., Edwards, T.W.D., 2008. A coupled isotope tracer method to characterize input water to lakes. J. Hydrol. 350, 1–13. https://doi.org/10.1016/j.jhydrol.2007.11.008.
Zemlyanitsina, L.A., 1970. Groudwaters of Lake basins of in-between Ishim-Irtysh Rivers. (In Russian). The Lakes of Semi-Arid Zone of the USSR. Nauka, Leningrad, pp. 49–74.
Zhang, M., Chen, Y., Shen, Y., Li, Y., 2017. Changes of precipitation extremes in arid Central Asia. Quat. Int. 436, 16–27. https://doi.org/10.1016/j.quaint.2016.12.024. Changes.